Shearing and Mixing Performance of Ultrahigh-Molecular-Weight Hydrolyzed Polyacrylamide (HPAM) Solution in a Helixes Static Mixer

Da-xing SUN, Wu-yi WANG, Ya-feng JU, Wen-ping SONG*,Yi-qing LI, Long-qiu LI*

Abstract: Static mixers have been widely used to dilute high viscosity, high-molecular-weight polymer mother liquor for polymer flooding, in which the mixing performance plays a critical role. In this work, a novel mixing configuration, named as Helixes static mixer, was proposed to reduce high viscosity degradation rate of polyacrylamide solution resulting from mechanical shear during mixing process. Computational fluid dynamics simulations along with experiments were performed to investigate the mixing process. Several criteria such as the intensity of segregation, mixing distance, pressure loss, and shear strain rate were used to evaluate the mixing and shear performance of static mixers. Compared to the SMX and Kenics static mixer, a longer mixing distance is needed for the Helixes static mixer to achieve an ideal mixture. A lower shear strain rate along with less viscosity degradation rate is obtained in flow field of Helixes static mixer. The spiral-lead and helical directions of mixing elements were optimized to improve mixing performance. Experimental results are in good agreement with the numerical simulations on the intensity of segregation. The viscosity degradation rate of HPAM solution which flows through Helixes static mixer is lower than that of SMX and Kenics static mixers.

Keywords: mixing performance; polymer flooding; shear strain rate; static mixer; viscosity degradation

1 INTRODUCTION

Partially hydrolyzed polyacrylamide (HPAM) solution with high viscosity and high molecular weight has been widely used in tertiary oil recovery [1]. During the preparation process, viscous polymer mother liquids have to be mixed with water using static mixers [2]. In the polymer flooding, the mixing and shear performance of static mixer is critical for the property of HPAM solution which concerns the efficiency and costs of oil recovery [3].

To improve mixing quality, many configurations which make fluid streams divided and redistributed sequentially, such as stacked lamella, helical inserts, curved pipe, and vortex generator, were designed [4]. The SMX and Kenics static mixers were applied for diluting, a non-Newtonian pseudoplastic fluid [5, 6], HPAM mother liquor in polymer flooding [7]. Experimental results showed that pseudoplastic fluid exhibits better mixing uniformity, lower pressure loss, and higher mixing efficiency than Newtonian fluid in SMX and Kenics static mixers [8-11]. The mixing performance of a high-viscosity fluid in several static mixers, such as Kenics static mixer with different number of twisted leaves, such as double, triple, multiple, and with different rotation directions, for example, right twist-type and spiral-type, has been investigated using computational fluid dynamics (CFD) calculations based on Lagrangian tracking method [12-15]. For these static mixers, the mixing performance can be enhanced by optimizing the longitudinal and angular positioning of mixing elements [16]. Overall, most of the previous works on static mixers focused on mixing quality or efficiency. The performance of static mixers was evaluated only by pressure drop, mixing distance, the Lyapunov exponent and the intensity of segregation. A few studies can be found studying the effect of shear strain rate on the viscosity of high-molecular-weight polymer solution.

Recently, the performance of a new-type mixer which combines SMX and Kenics static mixers is investigated by Zhang et al. [17] experimentally.They found that the combination of static mixer has a good mixing performance while the viscosity degradation rate of the effluent increases with the increase in flow rate. In oilfield application, viscosity reduction of displacement fluid caused by shear degradation in the SMX and Kenics static mixers is usually reported. The reason is that when the solution travels through the static mixers, velocity gradient generated by the static mixers produces a shearing action on the solution, so that the macromolecular chains of HPAM solution begin to fracture. In addition, as reported by Zaitounet al.[18], the complex flow configuration of static mixers will be accompanied with a larger shear strain rate during the mixing process. Especially, HPAM mother liquor with high concentration is more susceptible to shear strain rate [19]. High viscosity is an essential property for HPAM solution in polymer flooding, which can be used to decrease the water-to-oil mobility ratio and thereby enhance oil recovery (EOR) [20-22]. However, most of previous studies focus on the improvement of static mixing efficiency [23, 24]. To the best of our knowlege, there is no work found to report in reducing the viscosity loss of the mixed non-Newtonian fluid while maintaining the mixing efficiency of the static mixer. Therefore, it is of great importance to design a new static mixer with low shear action and high mixing efficiency to improve the displacement efficiency of the mixed liquid.

In this work, a Helixes static mixer was proposed to deal with high viscosity degradation rate during mixing process. CFD simulation was performed to assess its performance, such as the intensity of segregation, the mixing distance, the pressure drop, and the shear strain rate, to evaluate the comprehensive performance including mixing quality, pressure loss, and shear strain rate distribution of the mixing flow field. Furthermore, the geometric parameters of the Helixes static mixer were optimized for adapting practical production.

2 MODELING
2.1 Governing Equations

The fluid flowing through a static mixer is a fully three-dimensional chaotic flow. For this steady incompressible flow, the mass conservation and the momentum equations can be written as follows:

$$\frac{\partial}{\partial x_j}\left(\rho U_j\right) = 0 \tag{1}$$

$$\frac{\partial \rho U_i}{\partial t} + \frac{\partial}{\partial x_j}\left(\rho U_i U_j\right) = -\frac{\partial p'}{\partial x_i} + \frac{\partial}{\partial x_j}\left[\mu\left(\frac{\partial U_i}{\partial x_j} + \frac{\partial U_j}{\partial x_i}\right)\right] + S_M \tag{2}$$

where ρ denotes the mass density, t is time, x_i denotes position vector component, U_i denotes velocity vector component, S_M is the sum of body forces, μ is the dynamic viscosity and p' is the modified pressure. The Speziale, Sarkar and Gatski-Reynolds stress model (SSG-RSM) is used for the case of non-linear flow and vortex flow [25, 26]. The transport equation for the turbulent kinetic energy can be expressed as follows:

$$\frac{\partial}{\partial t}\left(\rho \overline{u_i u_j}\right) + \frac{\partial}{\partial x_k}\left(U_k \rho \overline{u_i u_j}\right) =$$
$$= P_{ij} + \phi_{ij} + \frac{\partial}{\partial x_k}\left[\left(\mu + \frac{2}{3}C_s \rho \frac{k^2}{\varepsilon}\right)\frac{\partial \overline{u_i u_j}}{\partial x_k}\right] - \frac{2}{3}\delta_{ij}\rho\varepsilon \tag{3}$$

where P_{ij} is the shear turbulence production term of the Reynolds stresses,

$$P_{ij} = -\rho \overline{u_i u_k}\frac{\partial U_j}{\partial x_k} - \rho \overline{u_j u_k}\frac{\partial U_i}{\partial x_k}$$

where ϕ_{ij} is the pressure-strain correlation, C_s is the Reynolds stress model constant (default value is 0.22), k is the turbulence kinetic energy, ε is the turbulence eddy dissipation, δ_{ij} is the Kronecker delta ($\delta_{ij} = 1$ if $i = j$, $\delta_{ij} = 0$ if $i \neq j$) and the Reynolds stresses were proposed as follows:

$$\rho \overline{u_i u_j} = \frac{2}{3}\delta_{ij}\left(\rho k + \mu\frac{\partial U_k}{\partial x_k}\right) - \mu\left(\frac{\partial U_i}{\partial x_j} + \frac{\partial U_j}{\partial x_i}\right) \tag{4}$$

For Newtonian fluids, the dynamic viscosity μ in Eq. (2), Eq. (3), and Eq. (4) is independent of the shear strain rate of the flow. However, for non-Newtonian fluids, the dynamic viscosity is a function of the shear strain rate. The dynamic viscosity in the Carreau Yasuda model is expressed as follows [27]:

$$\mu = \mu_\infty + \frac{\mu_0 - \mu_\infty}{\left[1 + (\lambda\dot{\gamma})^\alpha\right]^{\frac{1-n}{\alpha}}} \tag{5}$$

where μ_0 denotes low shear viscosity, μ_∞ is high shear viscosity, λ is time constant, $\dot{\gamma}$ denotes shear strain rate, n is power law index and α is Yasuda exponent. μ_0, μ_∞, λ, n, and α used in Eq. (5) can be found in Tab. 1 [28].

Table 1 Rheological properties of HPAM solutions

n	α	μ_0 / Pa·s	μ_∞ / Pa·s	λ
0.5	2	0.2	0	1

2.2 Computational Domain and Meshing

Fig. 1 shows the isometric views of the flow configurations for three static mixers, namely, SMX,

Kenics, and Helixes. Each static mixer consists of a pipe with an inner diameter of $D = 60$ mm and the pipe is fitted by several mixing elements. There are two inlets for HPAM mother solution and water, respectively. As shown in Fig. 1a, the SMX static mixer is composed of ten tandem elements, which is made of stacked lamella. Each element is rotated by 90 degrees relative to the previous one [29]. Fig. 1b shows that the mixing elements in the Kenics static mixer consist of eight tandem twisted plates. The leading edge and trailing edge of adjacent twisted plates are perpendicular [30]. The helical direction of adjacent twisted plates is opposite. Fig. 1c shows the Helixes static mixer proposed in this study, which is composed of seven parallel uninterrupted twisted tapes with the same spiral-lead $L = 30$ mm. The helical directions of seven twisted tapes are shown in the blow-ups of Fig. 1c, helical direction of the red twisted-tape is clockwise while the blue one is anticlockwise. Other geometric parameters of mixing elements are shown in the blow-ups of Fig. 1.
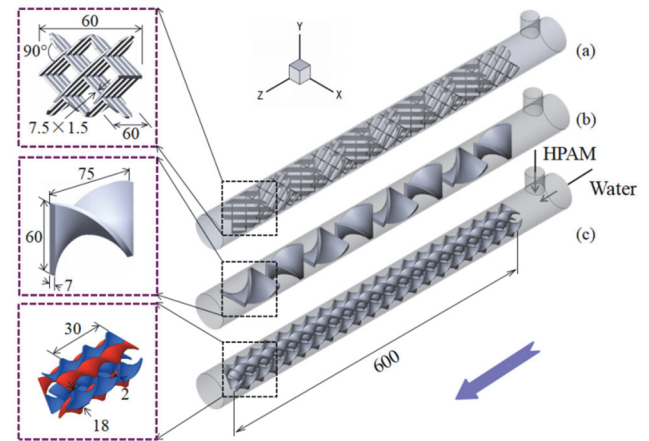

Figure 1 (a) Isometric view of the SMX static mixer, (b) isometric view of the Kenics static mixer and (c) isometric view of the Helixes static mixer

A non-uniform unstructured tetrahedral mesh was generated in commercial software, ANSYS ICEM 14.5. The "Octree" meshing method which is based on the spatial subdivision algorithm was used. This method ensures refinement of the mesh where necessary, however maintains large elements where possible, allowing for fast computation. The mesh convergence was performed by increasing mesh densities until the change of result is negligible. For the optimized mesh density, the grid cell size near the boundary of flow is no more than 0.2 mm, and the number of cells for these flow fields ranges from 3.5×10^6 to 3.8×10^6.

2.3 Numerical Calculation

To investigate the mixing process of HPAM mother solution and water in static mixers, the CFD code ANSYS CFX-14.5 was employed, which solved Navier-Stokes equations through a finite volume approximation [31, 32]. Higher-order upwind scheme was used to minimize the numerical diffusion. To discretize the advection terms of the governing equations, a high-resolution scheme of second-order approximation was used in this work. The root mean square (RMS) residual value of 10^{-5} was used for evaluating the convergence. No-slip boundary condition was applied for all solid boundaries. The velocity

at the inlets was assumed to be constant, while the static pressure at the outlet was assigned to be zero. The ratio of the flow rate of HPAM mother liquor and water was chosen to be 1/2. The flow of the static mixer was set to be 75 m³/d (i.e., the flow rate of HPAM mother liquor and water is $Q_{HPAM} = 25$ m³/d and $Q_{water} = 50$ m³/d, respectively). Thus, the speed of HPAM mother liquor and water at inlets was set to be 0.409 m/s and 0.204 m/s, respectively [33]. Properties of the HPAM mother liquor are shown in Tab. 2.

Table 2 Characterization of HPAM mother liquor

Molar mass	$M_r = 1.9 \times 10^7$ g/mol
Density	$\rho = 1320$ kg/m³
Dynamic viscosity	$\mu = 0.2$ Pa·s

3 NUMERICAL RESULTS AND DISCUSSION
3.1 Evaluation of Mixing and Shear Performance

Fig. 2a shows the HPAM volume fraction for three different static mixers, namely, SMX, Kenics, and Helixes static mixer. It is observed from Fig. 2a that the inlets with highest and lowest values of HPAM volume fraction correspond to inlets of HPAM mother liquor and water, respectively. In the regions at downstream side of the dashed lines, the HPAM volume fraction tends to be constant. It indicates that the HPAM mother liquor and water in these regions have been mixed completely. We can also observe that a good uniformity is reached for the SMX static mixer within a mixing distance of 147 mm while for the Kenics and Helixes static mixers, the mixing distance of HPAM mother liquor and water is 255 and 245 mm, respectively. This indicates that the mixing efficiency of SMX static mixer is higher than that of Kenics and Helixes static mixers.

In order to quantify the mixing performance of static mixers, intensity of segregation I_s at the Z direction was defined by Danckwerts in the following [34]:

$$I_s(Z) = \frac{\frac{1}{m-1}\sum_{i=1}^{m}\left[\varphi_Z(i) - \overline{\varphi_Z}\right]^2}{\overline{\varphi_Z}\left(1 - \overline{\varphi_Z}\right)} \qquad (6)$$

where $\varphi_Z(i)$ is a local value of HPAM volume fraction at a point i which is located in a given cross section of axial coordinate Z, $\overline{\varphi_Z}$ is the area-weighted average value of HPAM volume fraction for a given cross section of axial coordinate Z, and m is the number of samplings. $I_s(Z)$ is the intensity of segregation, referred to as segregation index, on a given cross section of axial coordinate Z. We can observe from Eq. (6) that the value of $I_s(Z)$ ranges from 0 to 1, corresponding to the status of ideal mixed and complete segregation, respectively.

Fig. 2b shows the intensity of segregation as a function of mixing distance for the three static mixers. We observe that the intensity of segregation decreases with an increase in mixing distance for all the three static mixers. This indicates that the mixture homogeneity increases with increasing the mixing distance. It can also be observed that the intensity of segregation for SMX static mixer is smaller than that of Kenics and Helixes static mixers for the same mixing distance. It means that the mixing quality of SMX

static mixer is better than that of Kenics and Helixes static mixers. This is because more frequently divided and redistributed mixture is made by stacked lamella in the SMX static mixer. As shown in Fig. 3, the motion pattern of mixture on cross section of SMX static mixer is more complex than that of Kenics and Helixes static mixers.
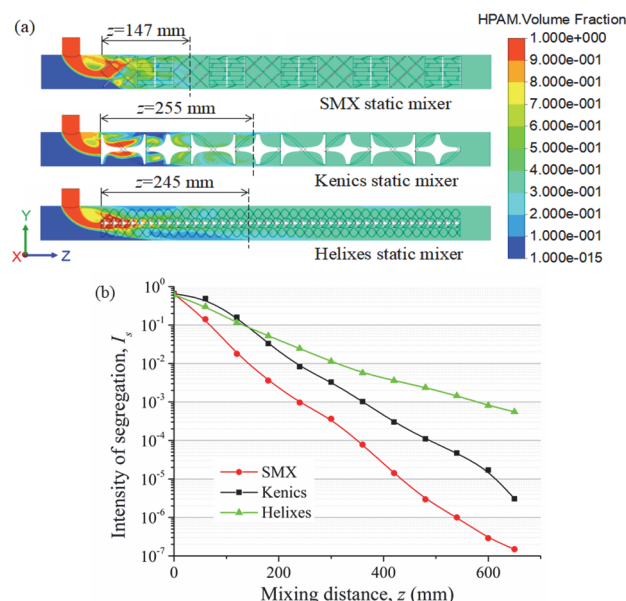

Figure 2 (a) Volume fraction distribution of HPAM mother liquor and (b) variation of the intensity of segregation I_s in Z direction for SMX, Kenics and Helixes static mixers for flow rate of HPAM mother liquor $Q_{HPAM} = 25$ m³/d, flow rate of water $Q_{water} = 50$ m³/d and $\mu = 0.2$ Pa·s
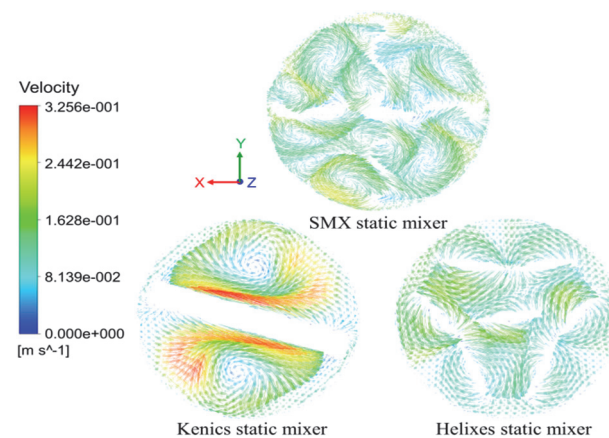

Figure 3 The motion pattern of mixture on cross section of SMX, Kenics and Helixes static mixers

As reported by Wong et al. [35], intensity of segregation of 10^{-3} has been used as the criteria for evaluating complete mixing. Note that the intensity of segregation for all the three static mixers satisfies the criteria for complete mixing.

As we all known, mixing quality enhancement may be accompanied with pressure loss which can be quantified using pressure drop shown as follows:

$$\Delta P(Z) = P_{in} - P(Z) \qquad (7)$$

where $P(Z)$ is the area-weighted pressure on a given cross section of axial coordinate Z and P_{in} is the pressure at the inlet.

The pressure distribution of SMX, Kenics, and Helixes static mixers is shown in Fig. 4. It can be observed that the pressure loss of SMX static mixer (2404.4 Pa) and Kenics static mixer (1261.9 Pa) is higher than that of Helixes static mixer (1046.5 Pa) at the same mixing distance of $Z = 600$ mm. Because the power consumption of static mixer is decided by pressure loss, the Helixes static mixer is relatively more energy saving.
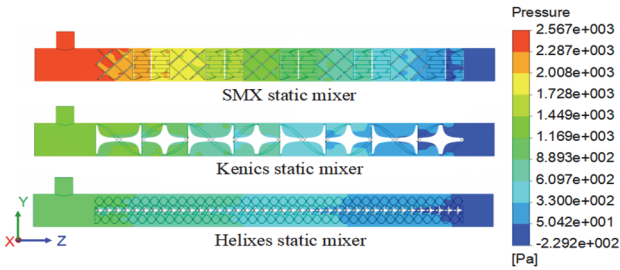

Figure 4 Pressure distribution for the SMX, Kenics and Helixes static mixers for $Q_{HPAM} = 25$ m³/d, $Q_{water} = 50$ m³/d, and $\mu = 0.2$ Pa·s

Moreover, the shear strain rate at a given point of the mixing flow field is defined as follows:

$$\gamma(x, y, z) = \left[2 \left\{ \left(\frac{\partial U_x}{\partial x} \right)^2 + \left(\frac{\partial U_y}{\partial y} \right)^2 + \left(\frac{\partial U_z}{\partial z} \right)^2 \right\} + \right.$$
$$\left. + \left(\frac{\partial U_x}{\partial y} + \frac{\partial U_y}{\partial x} \right)^2 + \left(\frac{\partial U_x}{\partial z} + \frac{\partial U_z}{\partial x} \right)^2 + \left(\frac{\partial U_y}{\partial z} + \frac{\partial U_z}{\partial y} \right)^2 \right]^{\frac{1}{2}} \quad (8)$$

where U_x, U_y, and U_z are the velocity vector components of fluid. HPAM solution is composed of long-chain macromolecules with shear sensitivity. The molecular chains are broken under the shear action, resulting in the decrease of viscosity in solution. However, the molecular conformation and molecular chain broken behavior are unable to be simulated in the macroscopic flow field. The viscosity loss caused by mechanical shear degradation cannot be directly expressed. In this work, we employed the shear strain rate distribution to demonstrate the strength of the shear action in static mixing flow field, thereby evaluating the viscosity reduction of the mixed solution.

Distribution of shear strain rate for the SMX, Kenics, and Helixes static mixers is shown in Fig. 5. As can be seen, the shear strain rate in Helixes static mixer is lower than that in SMX and Kenics static mixers. It can be observed from this figure that the regions of high shear strain rate occur at locations with similar characteristics. In SMX static mixer, the high shear regions are located near the junctions and intersections among stacked lamellas. In Kenics static mixer, the high shear regions are located around joints between neighboring mixing elements. And this is why the continuous, no tandem, helixes mixing element is chosen in our design. For Helixes static mixer, the shear strain rate is lower than that of SMX and Kenics static mixers. Only the shear strain rate at the inlet is slightly larger. The maximum and mean shear strain rate for three different static mixers is obtained and summarized in Tab. 3.

Table 3 Shear strain rate of three different static mixers.

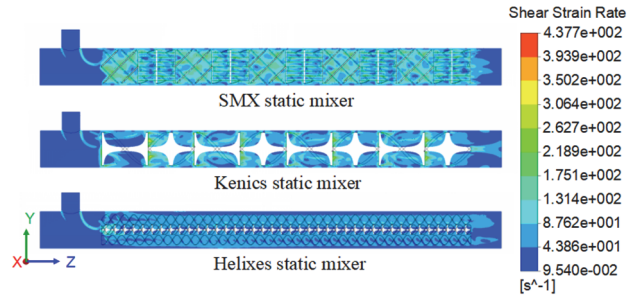| Shear strain rate	SMX	Kenics	Helixes
Maximum value	$\gamma_{max} = 341.4$ s⁻¹	$\gamma_{max} = 437.7$ s⁻¹	$\gamma_{max} = 243.3$ s⁻¹
Mean value	$\bar{\gamma} = 81.6$ s⁻¹	$\bar{\gamma} = 60.2$ s⁻¹	$\bar{\gamma} = 46.5$ s⁻¹

Figure 5 Shear strain rate distribution in the SMX, the Kenics and the Helixes static mixers for $Q_{HPAM} = 25$ m³/d, $Q_{water} = 50$ m³/d, and $\mu = 0.2$ Pa·s

We can observe from Tab. 3 that the maximum shear strain rate of Helixes static mixer is 243 s⁻¹, which is 28.7% and 44.4% smaller than that of SMX and Kenics static mixers, respectively. The mean shear strain rate of Helixes static mixer is 46.5 s⁻¹, which is 43.1% and 22.8% smaller than that of SMX and Kenics static mixers. It can be concluded that the Helixes static mixer displays lower shear action, compared to SMX and Kenics static mixers. This is because when fluid is flowing through the junctions and crossed geometry of SMX and Kenics static mixers, the flow direction and velocity are changed abruptly, leading to intensified local shear strain rate. During this process, polyacrylamide coils and molecule chains withstand higher tension and shear, which cause chains separation and breakage, ultimately resulting in a decrease of viscosity. Fig. 3 shows the radial flow path of mixing liquid on a cross section of Helixes static mixer. The rotational flow arises around each twisted-tape, and the radial flow among several twisted-tapes is induced by centrifugal force. Compared to the scissors-like structure of stacked lamellas and junctions of SMX and Kenics static mixers, the Helixes static mixer with parallel uninterrupted twisted-tapes has a fluid radial flow avoiding the mandatory segmentation and shear. Thus, the shear action from Helixes static mixer is smaller than that of SMX and Kenics static mixers.

3.2 Optimization of Mixing Element Geometries

As discussed in section 3.1, the mixing performance is directly related to the geometric parameters of mixing elements. Optimization for proper geometric parameters is needed for high mixing quality and low shear strain rate. For a Helixes static mixer, these parameters such as spiral-lead L and helical directions HD are shown in Fig. 6.
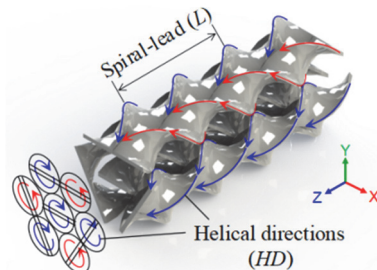

Figure 6 Optimizable geometric parameters of mixing element of a Helixes static mixer

The HPAM volume fraction for the Helixes static mixers with different spiral-lead is represented in Fig. 7. The spiral-leads are chosen to be 30, 60, 80, 100, and 140

mm, respectively. In the regions at downstream side of the dashed lines, the HPAM mother liquor and water were mixed completely. As can be seen, the larger the spiral-lead, the longer mixing distance is needed for complete mixing. It means that the mixing quality is enhanced with decreasing the spiral-lead of mixing elements.
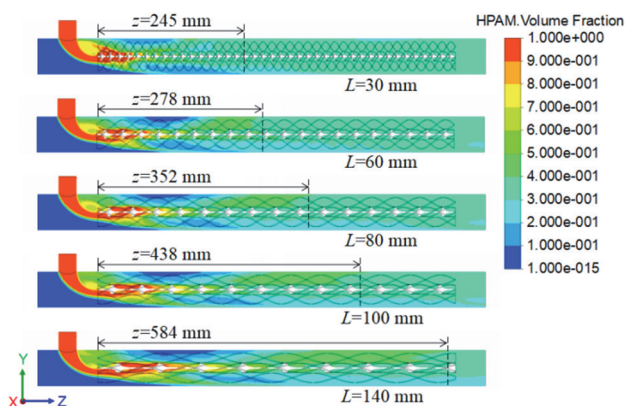

Figure 7 HPAM volume fraction distribution for the Helixes static mixers with different spiral-lead L for $Q_{HPAM} = 25$ m³/d, $Q_{water} = 50$ m³/d and $\mu = 0.2$ Pa·s
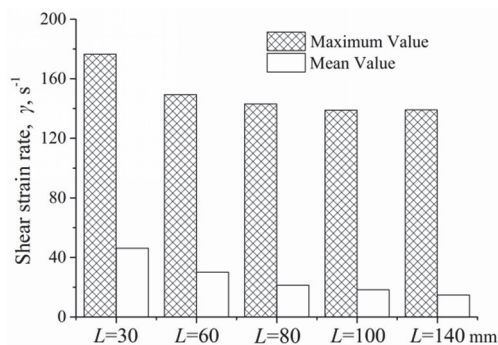

Figure 8 Maximum and mean value of shear strain rate for the Helixes static mixers with different spiral-lead L for $Q_{HPAM} = 25$ m³/d, $Q_{water} = 5\,0$ m³/d and $\mu = 0.2$ Pa·s
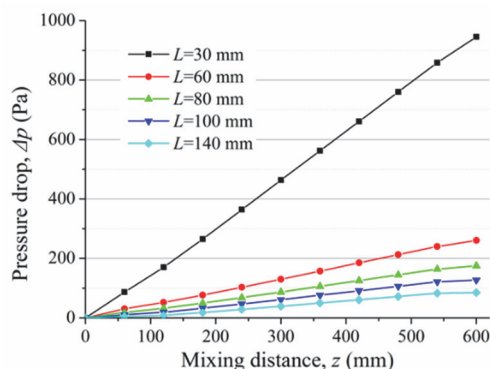

Figure 9 Variation of the pressure drop Δp in Z direction for the Helixes static mixers with different spiral-lead L for $Q_{HPAM} = 25$ m³/d, $Q_{water} = 50$ m³/d and $\mu = 0.2$ Pa·s

However, high mixing quality may accompany an increase of shear strain rate and thereby pressure loss. Just as Fig. 8 shows, both the maximum and mean value of shear strain rate of the Helixes static mixers increase with decreasing the spiral-lead of mixing elements. In addition, the variation of the pressure drop for different spiral-leads is shown in Fig. 9. As expected, higher pressure loss is obtained for the static mixer with a smaller value of spiral-lead. It can be observed that when spiral-lead is 30 mm, the

growth rate of pressure loss is significantly higher than that larger than 30 mm, namely, 60, 80, 100, and 140 mm. So that a larger spiral-lead can reduce pressure loss and shear strain rate with a decrease of mixing quality. Hence, on the premise of meeting requirement of mixing quality, a larger spiral-lead should be chosen.

Another essential factor which affects mixing process is the helical direction (*HD*) of mixing elements. It can be observed from Fig. 3 that the *HD* of mixing elements has a significant effect on the radial flow in Helixes static mixer. Meanwhile, the flow velocity and direction are asymmetric on cross section. Fig. 10a shows schematic of helical direction for four different configurations, R_A, R_B, R_C, and R_D. Fig. 10b shows the intensity of segregation as a function of mixing distance for these four configurations. It can be observed that the mixing quality of configuration R_D is obviously lower than others. We can also observe that the mixing quality of R_B presents a better mixing quality. This is because R_B makes fluid streams divided and converged evenly compared with R_C and R_D, and diminishes the effects of a higher local HPAM volume fraction caused by HPAM mother liquor which is lateral flow into water current on mixing quality compared with R_A. Moreover, the influences from *HD*s on the pressure loss and shear strain rate during the mixing process can be neglected. Thus, the R_B configuration is applicable to the Helixes static mixer.
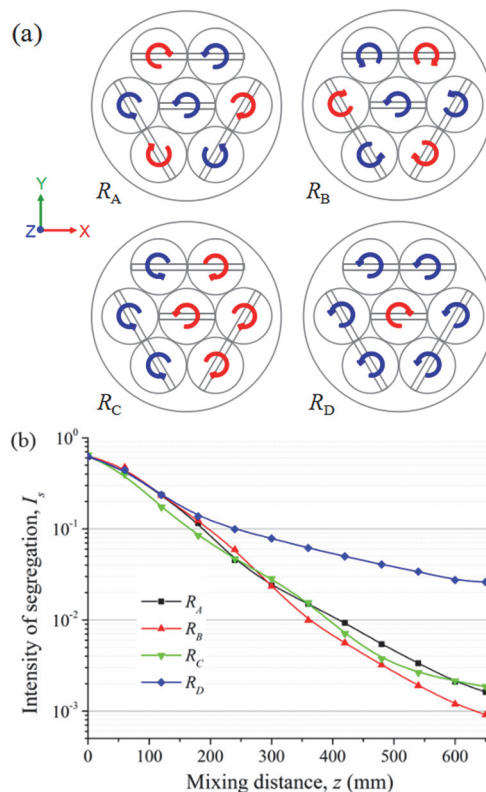

Figure 10 (a) Helical directions of each element and (b) variation of the intensity of segregation I_s in Z direction of four different configurations for $Q_{HPAM} = 25$ m³/d, $Q_{water} = 50$ m³/d and $\mu = 0.2$ Pa·s.

4 EXPERIMENTAL RESULTS AND DISCUSSION

The partially hydrolyzed polyacrylamide powder (HPAM19) was used in this study with the nominal molecular weight of 19×10^6 g/mol, and with the

hydrolysis of 25.3%. The polymer supplied by Daqing Oilfield Co., Ltd. is widely used in EOR.

The polymer was dissolved in deionized water with 2 wt% KCl and 400 mg/L NaN₃ (long-term solution conservation). An HPAM mother liquor at a concentration of 4000 mg/L was prepared by slowly adding the polymer powder to the shoulder of the vortex of the solvent while maintaining stirring using a paddle mixer. The paddle speed was 200 rpm at first, and was decreased to 100 rpm after 1 h of polymer addition for 5 h to ensure complete dissolution.

The schematic of experiments set-up is shown in Fig. 11. A liquid metering pump of diaphragm type was used to pump HPAM mother liquor to avoid a strong shear action on polymer solution before the mixing process. In order to investigate the conformance between the numberical model and reality, the static mixers with five different spiralleads of 30, 60, 80, 100, and 140mm were used in experiments, according to the previous simulations (Refer to Fig. 7).
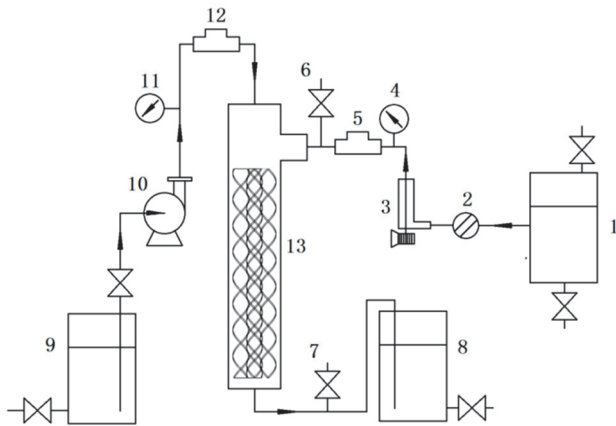

Figure 11 Flowsheet of experimental setup: 1-HPAM mother liquor tank; 2-strainer; 3, 10-liquid metering pump; 4, 11-pressure indicators; 5, 12-safty valve; 6, 7-sampling points; 8-product tank; 9- the distillated water tank; 13-static mixer

The flow rate of HPAM liquor and water at the inlet of static mixer is 25 m³/d and 50 m³/d, respectively. During the mixing process, the concentration and viscosity of several samples of mixture collected from sampling point No.8 were tested by spectrophotometer (Shanghai-Jinghua Type-722) and viscometer (Brookfield DV-II), respectively.

HPAM volume fraction is equivalent to the concentration of sample divided by the concentration of HPAM mother liquor, so that intensity of segregation of effluent mixture can be integrated from Eq. (6) as follow:

$$I_{sef} = \frac{\frac{1}{n-1}\sum_{j=1}^{n}\left[C_{ef}(j) - \overline{C_{ef}}\right]^2}{\overline{C_{ef}}\left(C_0 - \overline{C_{ef}}\right)} \quad (9)$$

where $C_{ef}(j)$ is the concentration of No. j sample of effluent mixture, $\overline{C_{ef}}$ denotes the average value of concentrations of all samples of effluent mixture, and n is the number of samples.

A comparison between numerical and experimental results for the intensity of segregation at outlets of five static mixers with different spiral-leads is shown in Fig.

12a. The experimental results show a good agreement with the numerical results on intensity of segregation.

Viscosity degradation rate can reflect the viscosity loss of HPAM solution, nevertheless, the numerical result does not include viscosity changes caused by mechanical degradation which is caused by shear strain rate. So that the changes of viscosity degradation rate in experiments and shear strain rate in numerical simulations with different spiral-leads are observed.

Viscosity degradation rate (DR) is calculated using the following equation:

$$DR = \left(\frac{\mu_{r0} - \mu_{ref}}{\mu_{r0} - 1}\right) \times 100\% \quad (10)$$

where μ_{r0} denotes the initial relative viscosity and μ_{ref} is the relative viscosity of the effluent mixture. Relative viscosity is the ratio of the HPAM solution viscosity to the solvent viscosity. The initial relative viscosity is the relative viscosity of the HPAM solution which is made with as low shear as possible, takes no account of time and efficiency, with the same concentration to the effluent mixture of static mixers.

Fig. 12b shows the maximum shear strain rate, mean shear strain rate and viscosity degradation rate as functions of spiral-lead. The maximum and mean shear strain rate show a similar changing tendency as that of the viscosity degradation rate. It is verified that during the static mixing process a decreased shear strain rate will reduce viscosity degradation and that the numerical results are able to reflect the shear action of reality and to be used to forecast the viscosity degradation rate.
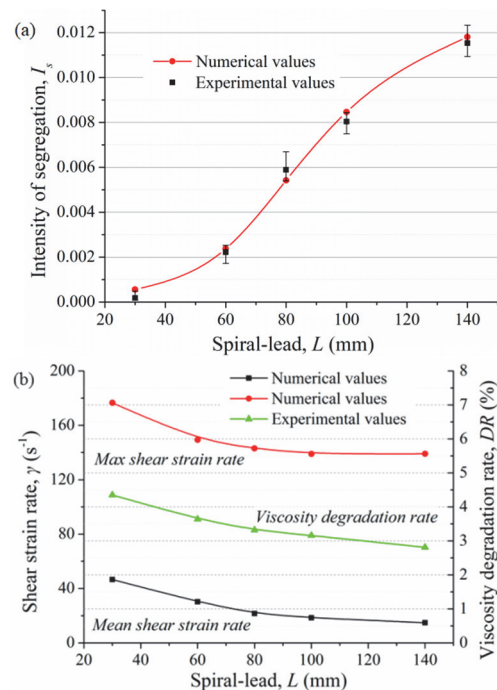

Figure 12 Comparisons between numerical and experimental results: (a) intensity of segregation and (b) shear strain rate and viscosity degradation rate.

In order to increase the efficiency and reduce the costs of oil recovery, the viscosity degradation rate of polymer solution should be less than 5%. The viscosity degradation rate of effluence of hundreds of SMX, Kenics, and Helixes static mixers which are used in oilfield is shown in Fig. 13.

We can observe that the average viscosity degradation rate of Helixes static mixers is lower than that of SMX and Kenics static mixers. Thus, the Helixes static mixer is of better viscosity degradation compared to other static mixers on the condition that it satisfies the mixing quality requirements.
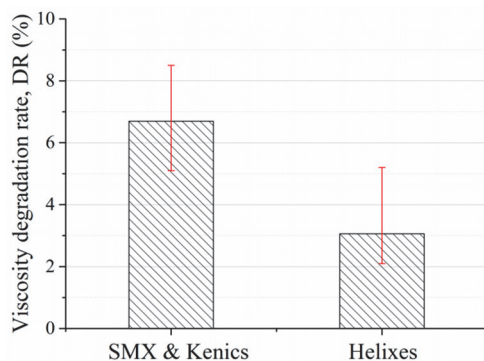

Figure 13 Viscosity degradation rate of SMX, Kenics and Helixes static mixers for a field experiment.

5 CONCLUSION

A novel static mixer, Helixes static mixer, used for diluting HPAM mother liquor in polymer flooding was proposed. Compared to the SMX and Kenics static mixer, a lower shear strain rate along with less viscosity degradation rate is obtained by Helixes static mixer. Optimizing of Helixes static mixer shows that a larger spiral-lead and helical directions of configuration R_B should be chosen to decrease viscosity degradation and energy consumption. Experiments agree with the numerical simulations and the viscosity degradation rate of HPAM solution flowing through Helixes static mixer which is lower than that flowing through SMX and Kenics static mixers.

Conflict of Interest

The authors declare that there are no other conflicts of interest.

6 REFERENCES

[1] Zhang, P., Wang, Y., Guo, S., Pan, B., Huang, W., Jia, Z., Zhou, C., Guo, M., & Yu, H. (2017). Seepage flow characteristics and ability for enhanced oil recovery based on ultra high molecular weight partially hydrolysed polyacrylamide. *International Journal of Oil, Gas and Coal Technology*, *14*(3), 216-231. https://doi.org/10.1504/ijogct.2017.10002915

[2] Wünsch, O. & Böhme, G. (2000). Numerical simulation of 3D viscous fluid flow and convective mixing in a static mixer. *Archive of Applied Mechanics*, *70*(1), 91-102. https://doi.org/10.1007/s004199900042

[3] Zhu, H., Luo, J., Klaus, O., & Fan, Y. (2012). The impact of extensional viscosity on oil displacement efficiency in polymer flooding. *Colloids and Surfaces A: Physicochemical and Engineering Aspects*, *414*, 498-503. https://doi.org/10.1016/j.colsurfa.2012.08.005

[4] Mickaily-Huber, E. S., Bertrand, F., Tanguy, P., Meyer, T., Renken, A., Rys, F. S., & Wehrli, M. (1996). Numerical simulations of mixing in an SMRX static mixer. *The Chemical Engineering Journal and the Biochemical Engineering Journal*, *63*(2), 117-126. https://doi.org/10.1016/ 0923-0467(96)03093-x

[5] Dejam, M. (2019). Advective-diffusive-reactive solute transport due to non-Newtonian fluid flows in a fracture surrounded by a tight porous medium. *International Journal of Heat and Mass Transfer*, *128*, 1307-1321. https://doi.org/10.1016/j.ijheatmasstransfer.2018.09.061

[6] Dejam, M. (2018). Dispersion in non-Newtonian fluid flows in a conduit with porous walls. *Chemical Engineering Science*, *189*, 296-310. https://doi.org/10.1016/j.ces.2018.05.058

[7] Rauline, D., Tanguy, P. A., Blévec, J. M. L., & Bousquet, J. (1998). Numerical investigation of the performance of several static mixers. *Canadian Journal of Chemical Engineering*, *76*(3), 527-535. https://doi.org/10.1002/cjce.5450760325

[8] Li, H. Z., Fasol, C., & Choplin, L. (1998). Residence time distribution of rheologically complex fluids passing through a sulzer SMX static mixer. *Chemical Engineering Communications*, *165*(1), 1-15. https://doi.org/10.1080/00986449808912367

[9] Liu, S., Hrymak, A. N., & Wood, P. E. (2006). Laminar mixing of shear thinning fluids in a SMX static mixer. *Chemical Engineering Science*, *61*(6), 1753-1759. https://doi.org/10.1016/j.ces.2005.10.026

[10] Fradette, L., Tanguy, P., Li, H.-Z., & Choplin, L. (2007). Liquid/Liquid viscous dispersions with a SMX static mixer. *Chemical Engineering Research & Design*, *85*(3), 395-405. https://doi.org/10.1205/cherd06206

[11] Mohammadi, A., Moghaddas, J., & Ariamanesh, A. (2015). Residence time and concentration distribution in a Kenics static mixer. *Chemical Engineering Communications*, *202*(2), 144-150. https://doi.org/10.1080/00986445.2013.832225

[12] Regner, M., Östergren, K., & Trägårdh, C. (2008). Influence of viscosity ratio on the mixing process in a static mixer: numerical study. *Industrial &Engineering Chemistry Research*, *47*(9), 3030-3036. https://doi.org/10.1021/ie0708071

[13] Thakur, R. K., Vial, C., Nigam, K. D. P., Nauman, E. B., & Djelveh, G. (2003). Static Mixers in the Process Industries: A Review. *Chemical Engineering Research & Design*, *81*(7), 787-826. https://doi.org/10.1205/0263876033322302968

[14] Meng, H., Wang, F., Yu, Y., Song, M., & Wu, J. (2014). A numerical study of mixing performance of high-viscosity fluid in novel static mixers with multitwisted leaves. *Industrial & Engineering Chemistry Research*, *53*(10), 4084-4095. https://doi.org/10.1021/ie402970v

[15] Meng, H., Song, M., Yu, Y., Wang, F., & Wu, J. (2015). Chaotic mixing characteristics in static mixers with different axial twisted-tape inserts. *Canadian Journal of Chemical Engineering*, *93*(10), 1849-1859. https://doi.org/10.1002/cjce.22268

[16] Habchi, C., & Harion, J. L. (2015). Enhanced mixing by optimized streamwise and angular positioning of longitudinal vorticity. *Applied Thermal Engineering*, *86*, 269-280.

https://doi.org/10.1016/j.applthermaleng.2015.04.039

[17] Zhang, L., Dong, J., Jiang, B., Sun, Y., Zhang, F., & Hao, L. (2015). A study of mixing performance of polyacrylamide solutions in a new-type static mixer combination. *Chemical Engineering and Processing*, *88*, 19-28. https://doi.org/10.1016/j.cep.2014.12.001

[18] Zaitoun, A., Makakou, P., Blin, N., Al-Maamari, R. S., Al-Hashmi, A.A. R., & Abdel-Goad, M. (2012). Shear stability of EOR polymers. *SPE Journal*, *17*(2), 335-339. https://doi.org/10.2118/141113-pa

[19] Al-Hashmi, A. A., Al-Maamari, R., Al-Shabibi, I., Mansoor, A., Al-Sharji, H., & Zaitoun, A. (2014). Mechanical stability of high-molecular-weight poly-acrylamides and an (acrylamido tert-butyl sulfonic acid)-acrylamide copolymer used in enhanced oil recovery. *Journal of Applied Polymer Science*, *131*(20), 40921. https://doi.org/10.1002/app.40921

[20] Sorbie, K. S. (1991). *Polymer-Improved Oil Recovery*. Edinburgh, UK: Springer Science & Business Media.

[21] Jung, J. C., Zhang, K., Chon, B. H., & Choi, H. J. (2013). Rheology and polymer flooding characteristics of partially hydrolyzed polyacrylamide for enhanced heavy oil recovery. *Journal of Applied Polymer Science*, *127*(6), 4833-4839. https://doi.org/10.1002/app.38070

[22] Saboorian-Jooybari, H., Dejam, M., & Chen, Z. (2016). Heavy oil polymer flooding from laboratory core floods to pilot tests and field applications: Half-century studies. *Journal of Petroleum Science and Engineering*, *142*, 85-100. https://doi.org/10.1016/j.petrol.2016.01.023

[23] Ghanem, A., Lemenand, T., Valle, D. D., & Peerhossaini, H. (2014). Static mixers: Mechanisms, applications, and characterization methods - A review. *Chemical Engineering Research & Design*, *92*(2), 205-228. https://doi.org/10.1016/j.cherd.2013.07.013

[24] Bayareh, M., Ashani, M. N., & Usefian, A. (2020). Active and passive micromixers: A comprehensive review. *Chemical Engineering and Processing*, *147*, 107771. https://doi.org/10.1016/j.cep.2019.107771

[25] Speziale, C. G., Sarkar, S., & Gatski, T. B. (1991). Modelling the pressure-strain correlation of turbulence: an invariant dynamical systems approach. *Journal of Fluid Mechanics*, *227*(1), 245-272. https://doi.org/10.1017/s0022112091000101

[26] Colombo, M. & Fairweather, M. (2015). Multiphase turbulence in bubbly flows: RANS simulations. *International Journal of Multiphase Flow*, *77*, 222-243. https://doi.org/10.1016/j.ijmultiphaseflow.2015.09.003

[27] Boyd, J., Buick, J. M., & Green, S. (2007). Analysis of the Casson and Carreau-Yasuda non-Newtonian blood models in steady and oscillatory flows using the lattice Boltzmann method. *Physics of Fluids*, *19*(9), 93103. https://doi.org/10.1063/1.2772250

[28] Vlassopoulos, D. & Schowalter, W. R. (1994). Steady viscometric properties and characterization of dilute drag‑reducing polymer solutions. *Journal of Rheology*, *38*(5), 1427-1446. https://doi.org/10.1122/1.550605

[29] Rauline, D., Le-Blévec, J.M., Bousquet, J., & Tanguy, P. A. (2000). A Comparative Assessment of the Performance of the Kenics and SMX Static Mixers. *Chemical Engineering Research & Design*, *78*(3), 389-396. https://doi.org/10.1205/026387600527284

[30] Galaktionov, O. S., Anderson, P. D., Peters, G. W. M., & Meijer, H. E. H. (2003). Analysis and optimization of Kenics static mixers. *International Polymer Processing*, *18*(2), 138-150. https://doi.org/10.3139/217.1732

[31] ANSYS CFX, 14.5, (2012).ANSYS, Canonsburg, http://www.ansys.com/products/fluids/ ansys-cfx.

[32] Hossain, S. & Kim, K.-Y. (2016). Parametric investigation on mixing in a micromixer with two-layer crossing channels. *SpringerPlus*, *5*(1), 794-794. https://doi.org/10.1186/s40064-016-2477-x

[33] Wang, J. & Liu, H. (2014). A novel model and sensitivity analysis for viscoelastic polymer flooding in offshore oilfield. *Journal of Industrial and Engineering Chemistry*, *20*(2), 656-667. https://doi.org/10.1016/j.jiec.2013.05.030

[34] Danckwerts, P. V. (1952). The definition and measurement of some characteristics of mixtures. *Flow Turbulence and Combustion*, *3*(4), 279-296. https://doi.org/10.1007/bf03184936

[35] Wong, S. H., Bryant, P., Ward, M., & Wharton, C. (2003). Investigation of mixing in a cross-shaped micromixer with static mixing elements for reaction kinetics studies. *Sensors and Actuators B-Chemical*, *95*(1), 414-424. https://doi.org/10.1016/s0925-4005(03)00447-7

Contact information:

Da-xing SUN, PhD candidate
State Key Laboratory of Robotics and System, Harbin Institute of Technology,
NO. 92 West Dazhi St., Nangang District,Harbin, Heilongjiang, China.
E-mail: sundaxing@yeah.net

Wu-yi WANG, Professor
State Key Laboratory of Robotics and System, Harbin Institute of Technology,
NO. 92 West Dazhi St., Nangang District,Harbin, Heilongjiang, China.
E-mail: wangwuyi@hit.edu.cn

Ya-feng JU, Senior Engineer
Oil & Gas Technology Research Institute of Petrochina Changqing Oilfiled Company,
Mingguang Road, Weiyang District,Xi'an, Shaanxi, China
E-mail**:** jyf_cq@petrochina.com.cn

Wen-ping SONG, Associate Professor
(Corresponding Author)
State Key Laboratory of Robotics and System, Harbin Institute of Technology,
NO. 92 West Dazhi St., Nangang District,Harbin, Heilongjiang, China.
E-mail: songwenping@hit.edu.cn

Yi-qing LI, Assistant engineer
State Key Laboratory of Robotics and System, Harbin Institute of Technology,
NO. 92 West Dazhi St., Nangang District,Harbin, Heilongjiang, China.
E-mail: liyiqing_hit@yeah.net

Long-qiu LI, Professor
(Corresponding Author)
1. State Key Laboratory of Robotics and System, Harbin Institute of Technology,
NO. 92 West Dazhi St., Nangang District,Harbin, Heilongjiang, China.
2. State Key Laboratory of Tribology, Tsinghua University.NO. 30 Shuangqing Road, Haidian District,
Peking, China
E-mail: longqiuli@hit.edu.cn